Short article

Cell Host & Microbe

Prior infection with SARS-CoV-2 boosts and broadens Ad26.COV2.S immunogenicity in a variant-dependent manner

Graphical abstract

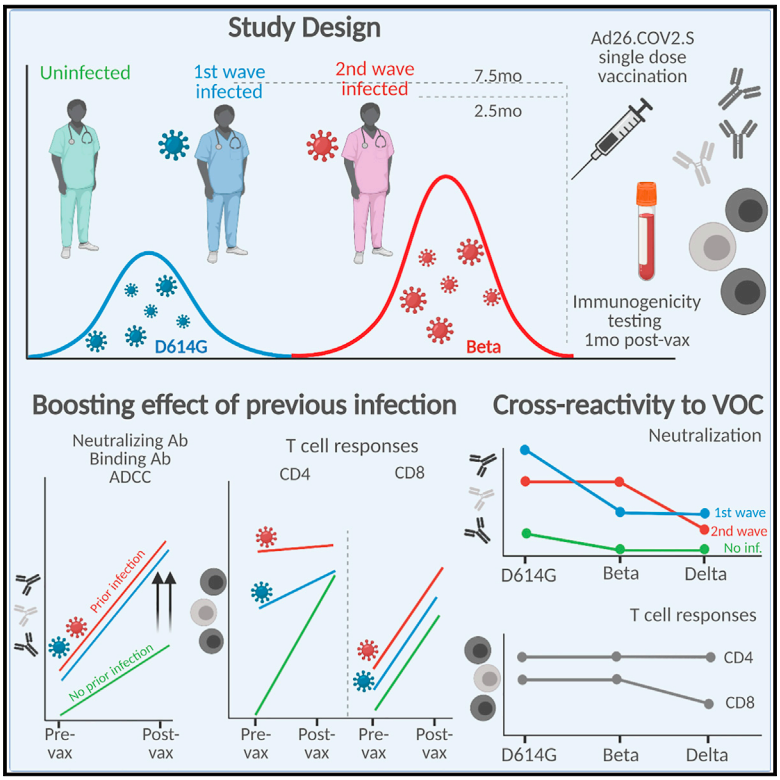

Highlights

- Infection before Ad26CoV2.S vaccination boosts binding, neutralization, and ADCC
- Antibody boosting is not affected by time between infection and vaccination
- Neutralization breadth for VOCs is determined by the sequence of the infecting virus
- T cell responses are moderately boosted by prior infection and cross-react with VOCs

Authors

Roanne Keeton, Simone I. Richardson, Thandeka Moyo-Gwete, ..., Ntobeko A.B. Ntusi, Penny L. Moore, Wendy A. Burgers

Correspondence

ntobeko.ntusi@uct.ac.za (N.A.B.N.), pennym@nicd.ac.za (P.L.M.), wendy.burgers@uct.ac.za (W.A.B.)

In brief

Keeton, Richardson, Moyo-Gwete, et al. show that SARS-CoV-2 infection prior to Ad26CoV2.S vaccination significantly boosts cross-reactive ADCC and binding and neutralizing antibodies and moderately boosts T cell responses against variants of concern. Furthermore, the infecting virus spike sequence determines the cross-reactivity of neutralizing responses, with implications for second-generation vaccine design.

Keeton et al., 2021, Cell Host & Microbe *29*, 1611–1619
November 10, 2021
https://doi.org/10.1016/j.chom.2021.10.003

CellPress

Cell Host & Microbe

CellPress

Short article

Prior infection with SARS-CoV-2 boosts and broadens Ad26.COV2.S immunogenicity in a variant-dependent manner

Roanne Keeton,[1,2,20] Simone I. Richardson,[3,4,20] Thandeka Moyo-Gwete,[3,4,20] Tandile Hermanus,[3,4,20] Marius B. Tincho,[1,2] Ntombi Benede,[1,2] Nelia P. Manamela,[3,4] Richard Baguma,[1] Zanele Makhado,[3,4] Amkele Ngomti,[1,2] Thopisang Motlou,[3,4] Mathilda Mennen,[5] Lionel Chinhoyi,[5] Sango Skelem,[5] Hazel Maboreke,[1,6] Deelan Doolabh,[1,2] Arash Iranzadeh,[1,2] Ashley D. Otter,[7] Tim Brooks,[7] Mahdad Noursadeghi,[8] James C. Moon,[9,10] Alba Grifoni,[11] Daniela Weiskopf,[11] Alessandro Sette,[11,12] Jonathan Blackburn,[1,6] Nei-Yuan Hsiao,[2,13] Carolyn Williamson,[1,2,14] Catherine Riou,[1,2,14] Ameena Goga,[15] Nigel Garrett,[16,17] Linda-Gail Bekker,[1,18] Glenda Gray,[15] Ntobeko A.B. Ntusi,[1,5,19,21,*] Penny L. Moore,[3,4,21,*] and Wendy A. Burgers[1,2,14,21,22,*]

[1]Institute of Infectious Disease and Molecular Medicine, University of Cape Town, Cape Town, South Africa
[2]Division of Medical Virology, Department of Pathology, University of Cape Town, Cape Town, South Africa
[3]National Institute for Communicable Diseases of the National Health Laboratory Services, Johannesburg, South Africa
[4]MRC Antibody Immunity Research Unit, School of Pathology, University of the Witwatersrand, Johannesburg, South Africa
[5]Department of Medicine, University of Cape Town and Groote Schuur Hospital, South Africa
[6]Division of Chemical and Systems Biology, Department of Integrative Biomedical Sciences, University of Cape Town, Cape Town, South Africa
[7]National Infection Service, Public Health England, Porton Down, UK
[8]Division of Infection and Immunity, University College London, London, UK
[9]Institute of Cardiovascular Sciences, University College London, London, UK
[10]Barts Heart Centre, St Bartholomew's Hospital, Barts Health NHS Trust, London, UK
[11]Center for Infectious Disease and Vaccine Research, La Jolla Institute for Immunology, La Jolla, CA, USA
[12]Department of Medicine, Division of Infectious Diseases and Global Public Health, University of California San Diego, La Jolla, CA, USA
[13]NHLS Groote Schuur Hospital, University of Cape Town, Cape Town, South Africa
[14]Wellcome Centre for Infectious Diseases Research in Africa, University of Cape Town, Cape Town, South Africa
[15]South African Medical Research Council, Cape Town, South Africa
[16]Centre for the AIDS Programme of Research in South Africa, Durban, South Africa
[17]Discipline of Public Health Medicine, University of KwaZulu-Natal, Durban, South Africa
[18]Desmond Tutu HIV Centre, Cape Town, South Africa
[19]Hatter Institute for Cardiovascular Research in Africa, Faculty of Health Sciences, University of Cape Town, Cape Town, South Africa
[20]These authors contributed equally
[21]These authors contributed equally
[22]Lead contact
*Correspondence: ntobeko.ntusi@uct.ac.za (N.A.B.N.), pennym@nicd.ac.za (P.L.M.), wendy.burgers@uct.ac.za (W.A.B.)
https://doi.org/10.1016/j.chom.2021.10.003

SUMMARY

The Johnson and Johnson Ad26.COV2.S single-dose vaccine represents an attractive option for coronavirus disease 2019 (COVID-19) vaccination in countries with limited resources. We examined the effect of prior infection with different SARS-CoV-2 variants on Ad26.COV2.S immunogenicity. We compared participants who were SARS-CoV-2 naive with those either infected with the ancestral D614G virus or infected in the second wave when Beta predominated. Prior infection significantly boosts spike-binding antibodies, antibody-dependent cellular cytotoxicity, and neutralizing antibodies against D614G, Beta, and Delta; however, neutralization cross-reactivity varied by wave. Robust CD4 and CD8 T cell responses are induced after vaccination, regardless of prior infection. T cell recognition of variants is largely preserved, apart from some reduction in CD8 recognition of Delta. Thus, Ad26.COV2.S vaccination after infection could result in enhanced protection against COVID-19. The impact of the infecting variant on neutralization breadth after vaccination has implications for the design of second-generation vaccines based on variants of concern.

INTRODUCTION

The Johnson and Johnson Ad26.COV2.S vaccine is a single-dose adenovirus 26-vectored vaccine expressing the severe acute respiratory syndrome coronavirus 2 (SARS-CoV-2) Wuhan-1 stabilized spike. A phase 3 clinical trial of Ad26.COV2.S on three continents demonstrated 66% efficacy against moderate disease and 85% protection against severe disease 28 days

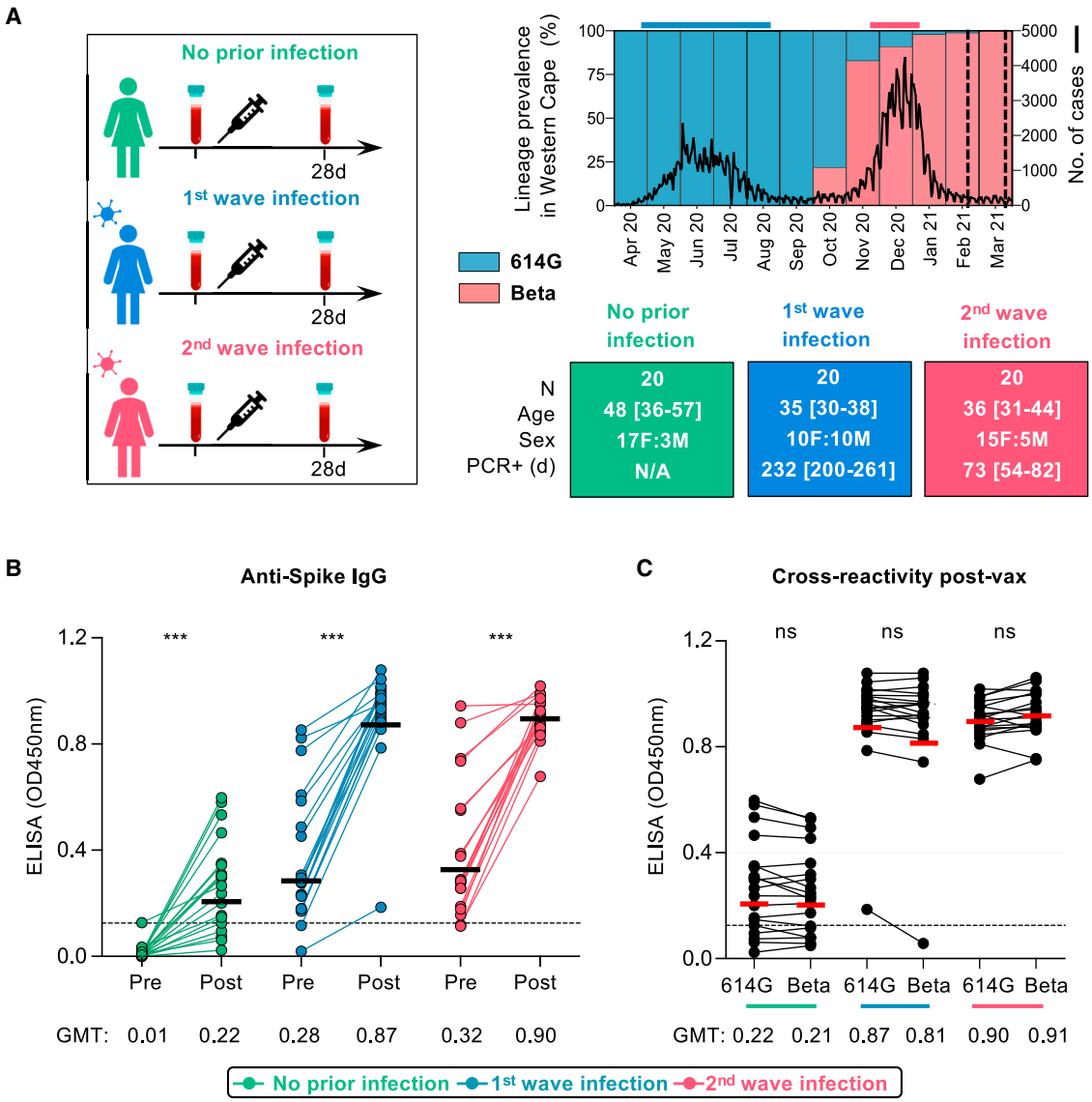

Figure 1. Spike-specific antibody responses in Ad26.COV2.S-vaccinated healthcare workers

(A) Study design showing three groups (left panel), either with no prior infection or infection in the first wave (May–August 2020) and infection in the second wave (November 2020–January 2021). Samples were taken pre-vaccination and one month after vaccination. SARS-CoV-2 epidemiological dynamics in the Western Cape (South Africa) are shown (top right panel). Prevalence of SARS-CoV-2 lineages is shown on the left y axis. The ancestral strain (D614G) is depicted in blue, and Beta is depicted in red. The number of COVID-19 cases is represented on the right y axis. The bars on top of the graph indicate the periods when participants were infected in the first and second waves. Vertical dotted lines indicate when vaccination occurred. Characteristics of participants in the three groups (bottom right panel). Sex, age (median and IQR), and days since PCR-confirmed infection.

(B) Plasma samples from participants with no prior infection (green, n = 19), first-wave infection (blue, n = 20), or second-wave infection (red, n = 19) were tested for binding to D614G spike protein pre- and post-vaccination (OD_{450nm}).

(C) Cross-reactivity of vaccine-induced antibody responses to D614G and Beta spike. The colored lines below the graph correspond with the key. The threshold for positivity is indicated by a dotted line. Horizontal bars indicate GMT, with values shown. Statistical analyses were performed with the Mann-Whitney test between groups, and the Wilcoxon test was performed for pre- and post-vaccine time points or D614G in comparison with Beta responses. ***$p < 0.001$.

after vaccination (Sadoff et al., 2021). Moreover, the South African arm of the trial showed similar levels of efficacy despite the emergence of the neutralization-resistant SARS-CoV-2 Beta variant. Vaccination with Ad26.COV2.S triggers neutralizing responses that gradually increase in magnitude and breadth, as well as potent antibody Fc effector functions and T cell activity, both of which retain activity against variants of concern (VOCs) (Moore et al., 2021; Barouch et al., 2021; Stephenson et al., 2021; Alter et al., 2021).

Prior infection boosts titers of binding and neutralizing antibodies elicited by mRNA vaccines (Manisty et al., 2021; Saadat et al., 2021; Stamatatos et al., 2021; Vanshylla et al., 2021; Wang et al., 2021b). These increased titers conferred the ability to neutralize SARS-CoV-2 VOCs, illustrating that only one dose of

these vaccines might be sufficient to protect previously infected individuals. Similarly, a single dose of the BNT162b2 vaccine boosted antibody-dependent cellular cytotoxicity (ADCC) in previously infected individuals, and T cell cross-reactivity was largely retained (Geers et al., 2021; Reynolds et al., 2021; Tauzin et al., 2021). The impact of prior infection on immune responses elicited by vectored vaccines is less well defined (Havervall et al., 2021), as is the impact of the duration between infection and vaccination, or the genotype of the infecting virus.

RESULTS

South Africa experienced a first wave of infections in mid-2020, dominated by the ancestral SARS-CoV-2 D614G variant. From November 2020 to February 2021, a second wave of infections was dominated by the Beta variant (Tegally et al., 2021; Wibmer et al., 2021; Cele et al., 2021; Wang et al., 2021a). We established an observational study of 400 healthcare workers (HCWs) with serial sampling since the first wave. We studied 60 HCWs who were vaccinated in a phase 3b implementation trial of single-dose Ad26.COV2.S vaccine (Takuva et al., 2021). HCWs were recruited into three groups, namely those never infected with SARS-CoV-2 (n = 20) and those with PCR-confirmed infection during the first wave (n = 20) or second wave (n = 20) (Figure 1A; Table S1). The Beta variant accounted for >90% of infections in the Western Cape in the second wave (Figure 1A), making it likely that this variant was responsible for infections in the latter group. Indeed, whole-genome sequencing of 8/20 second-wave participants confirmed infection with Beta. Serological profiles were generated for each participant by measuring nucleocapsid and spike antibodies since July 2020 (3–8 monthly visits) (Figures S1A–S1C). These data confirmed the absence of infection (or re-infection), and the timing of first- or second-wave infection. We identified one potential vaccine breakthrough infection and one suspected re-infection, both excluded from subsequent analyses.

Peripheral blood mononuclear cells (PBMCs) and plasma were collected prior to vaccination (median 22 days, interquartile range (IQR) 14–29) and approximately one month after vaccination (median 29 days, IQR 28–34). We tested pre- and post-vaccination plasma for immunoglobulin (Ig)G binding antibodies to the ancestral D614G spike. Binding antibodies elicited by vaccination in the absence of infection (geometric mean titer [GMT]: 0.22) were comparable with those in both infected groups prior to vaccination (GMT: 0.28 and 0.32 for first and second wave, respectively). However, vaccination in HCWs with prior infection in both waves resulted in binding responses being boosted 3-fold, to a GMT of 0.87 or 0.9 for the first and second waves, respectively (Figure 1B). In all HCWs, regardless of prior infection, spike-specific binding antibodies were cross-reactive, with no significant difference in binding between the D614G and Beta spike (Figure 1C).

By using a SARS-CoV-2 pseudovirus assay with the D614G spike, we tested neutralizing antibodies elicited by vaccination alone. Consistent with previous studies (Moore et al., 2021), we saw low titers post-vaccination in the infection-naive group (GMT: 74). In both groups with prior infection, we observed a significant boost in neutralization after vaccination against D614G and Beta (Figure 2A; Figure S2A). For first-wave HCWs, titers were boosted 13-fold from a GMT of 210 to 2,798 (Figure 2A). Second-wave HCWs were boosted 12-fold from a GMT of 99 to 1,157. To determine cross-reactivity of neutralizing antibodies, we compared neutralization of D614G with Beta and Delta. For antibodies induced by vaccination alone, all participants showed significantly lower titers against Beta (85% showing no neutralization, GMT: 28) and Delta (78% showing no neutralization, GMT: 29). In both groups of previously infected HCWs, we saw cross-neutralization of Beta and Delta, but the degree of cross-reactivity varied by wave of infection (Figures 2B and 2C). For HCWs infected in the first wave, although neutralization of Beta and Delta was maintained, titers were significantly lower for both VOCs (a reduction in GMT from 2,798 to 606 and 443, respectively, compared to those for D614G). In contrast, plasma from those infected in the second wave with Beta showed no significant difference in neutralization of D614G (GMT: 1157) but 6-fold lower neutralization of Delta (GMT: 200, $p < 0.001$) (Figures 2B and 2C). Overall, prior infection followed by vaccination triggered high-titer neutralizing antibodies able to neutralize VOCs. However, the pattern of neutralization varied by wave, suggesting that the neutralizing antibody repertoire was shaped by the genotype of the infecting variant.

To assess the impact of prior infection on Fc effector responses to vectored vaccines is unknown. We measured the ability of plasma antibodies to cross-link FcγRIIIa (CD16)-expressing cells and cell surface D614G, Beta, or Delta spikes on target cells, as a surrogate for ADCC. In previously infected individuals, post-vaccination responses after both waves were significantly higher against D614G, Beta, and Delta (Figure 3A; Figure S2B), closely mirroring the fold increases of spike binding titers (Figure 1B). However, responses to D614G elicited by vaccination alone (GMT: 39) were similar to those elicited by infection (GMT: 86 for first wave and 54 for second wave) (Figure 3A; Figure S2B). ADCC assays performed with the Beta and Delta variants showed no significant loss in activity when compared to D614G in the vaccine-only group (Figure 3B) or in individuals with prior infection (Figures 3B and 3C), demonstrating cross-reactive ADCC responses to VOCs.

We examined the effect of prior SARS-CoV-2 infection on vaccine T cell responses. We measured intracellular cytokine production (interferon [IFN]-γ, tumor necrosis factor [TNF]-α, and interleukin [IL]-2) in response to peptides covering the Wuhan-1 spike (Figure S3A). Vaccination induced spike-specific CD4 and CD8 T cell responses in all groups (Figures 4A and 4B). Infection-naive participants or those infected in the first wave had significantly higher CD4 T cell responses after vaccination (median: 0.051 and 0.064, respectively). The second-wave group had pre-existing responses that were significantly higher than the first-wave baseline infection responses and mounted a more modest response to vaccination, with similar medians (0.132% and 0.147%, p = not significant [ns]). CD8 responses were present in fewer individuals prior to vaccination (15 and 32%, versus 85 and 100% for CD4 responses in first- and second-wave groups, respectively) and did not differ significantly between the groups (Figure 4B; Figure S3B). Median CD4 T cell frequencies from pre- to post-vaccination decreased with higher magnitude of pre-existing responses, with a 5.7-fold change in the infection-naive group, 1.5-fold in the first-wave group, and 1.1-fold in the second-wave group. For CD8 responses, the fold increase was similar for the three

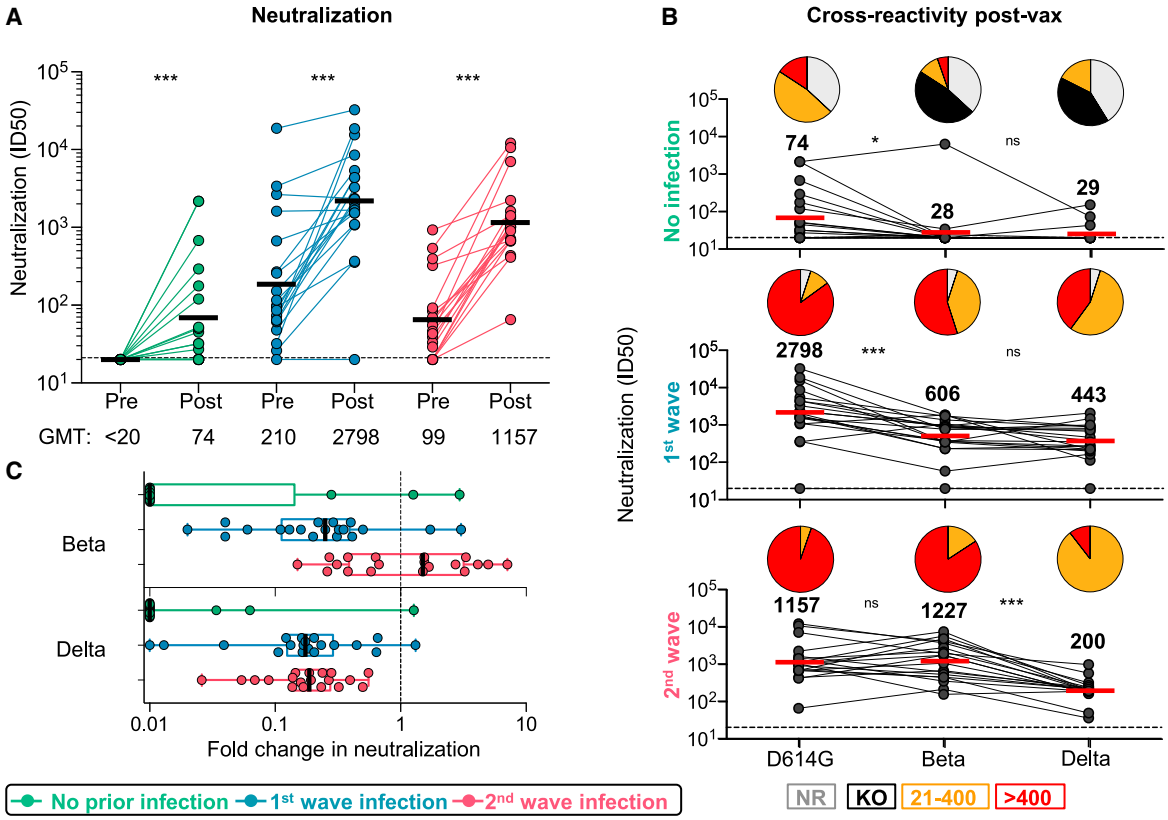

Figure 2. Neutralizing antibody responses to Ad26.COV2.S vaccination

(A) Neutralization of the SARS-CoV-2 D614G pseudovirus by plasma pre- and post-vaccination from participants with no prior infection (green, n = 19) and those infected in the first (blue, n = 20) and second waves (red, n = 19). Neutralization is reflected as an ID_{50} titer. The threshold for positivity is indicated by a dotted line

(B) Cross-reactive neutralization post-vaccination against D614G, Beta, and Delta. Pie charts show the proportion of vaccine non-responders (NR; gray), knockout of neutralization of Beta or Delta (KO; black), and the titer of 20–400 (orange), or >400 (red). The horizontal bars indicate GMT, with values indicated. Statistical analyses were performed with the Friedman test between groups and the Wilcoxon test for paired analyses. *$p < 0.05$, ***$p < 0.001$.

(C) Fold change of post-vaccination D614G neutralization titers relative to Beta or Delta. The vertical bars indicate median fold change with error bars for IQR.

groups (Figure 4C). A greater proportion of individuals mounted a CD4 response than to a CD8 response (Figure 4C). Polyfunctional profiles of vaccine responses demonstrated that CD4 T cells had the capacity to produce multiple cytokines simultaneously, whereas CD8 T cells produced predominantly IFN-γ alone (Figure S3C), with no significant difference in the profiles after vaccination for those who were infection naive to those with prior infection.

Finally, we assessed whether T cells induced by vaccination recognized Beta and Delta. We tested spike peptides corresponding to the viral sequences of the ancestral strain, Beta, or Delta in 24 vaccinees. CD4 T cell recognition of Beta or Delta was fully preserved, compared to the ancestral strain (Figure 4D). Spike-specific CD8 T cells (in 15/24 participants) cross-recognized Beta spike in 14/15 responders. In contrast, the median magnitude of the cytokine response was significantly lower against Delta than against Beta ($p = 0.041$), and 8/15 (53%) of CD8 responders had a 2-fold or greater reduction in the response to Delta, including five with complete loss of recognition (Figure 4D). Overall, these results demonstrate that robust CD4 and CD8 T cell responses are generated after vaccination, regardless of prior infection. Vaccine T cell cross-recognition of variants is largely preserved, with the exception of a reduced ability for CD8 recognition of Delta in some vaccinees.

DISCUSSION

Several mRNA vaccines have demonstrated a boosting effect of prior infection (Manisty et al., 2021; Reynolds et al., 2021; Saadat et al., 2021; Stamatatos et al., 2021; Wang et al., 2021b). However, whether this is true of viral vectors, including the single-dose Johnson and Johnson vaccine, is unclear. We show that infection prior to vaccination with Ad26.COV2.S significantly boosts the magnitude and cross-reactivity of binding antibodies, neutralizing antibodies, and Fc effector function. T cell responses were robustly generated even in the absence of prior infection and were preserved against Beta. These data have particular significance in countries like South Africa, where SARS-CoV-2 seropositivity is 20%–40% (Mutevedzi et al., 2021; Hsiao et al., 2020; Sykes et al., 2021). Thus, prior infection could enhance the protective efficacy of this vaccine, which is frequently used in settings with limited resources.

Neutralization breadth was shaped by the variant responsible for infection. Prior exposure to D614G resulted in reduced titers

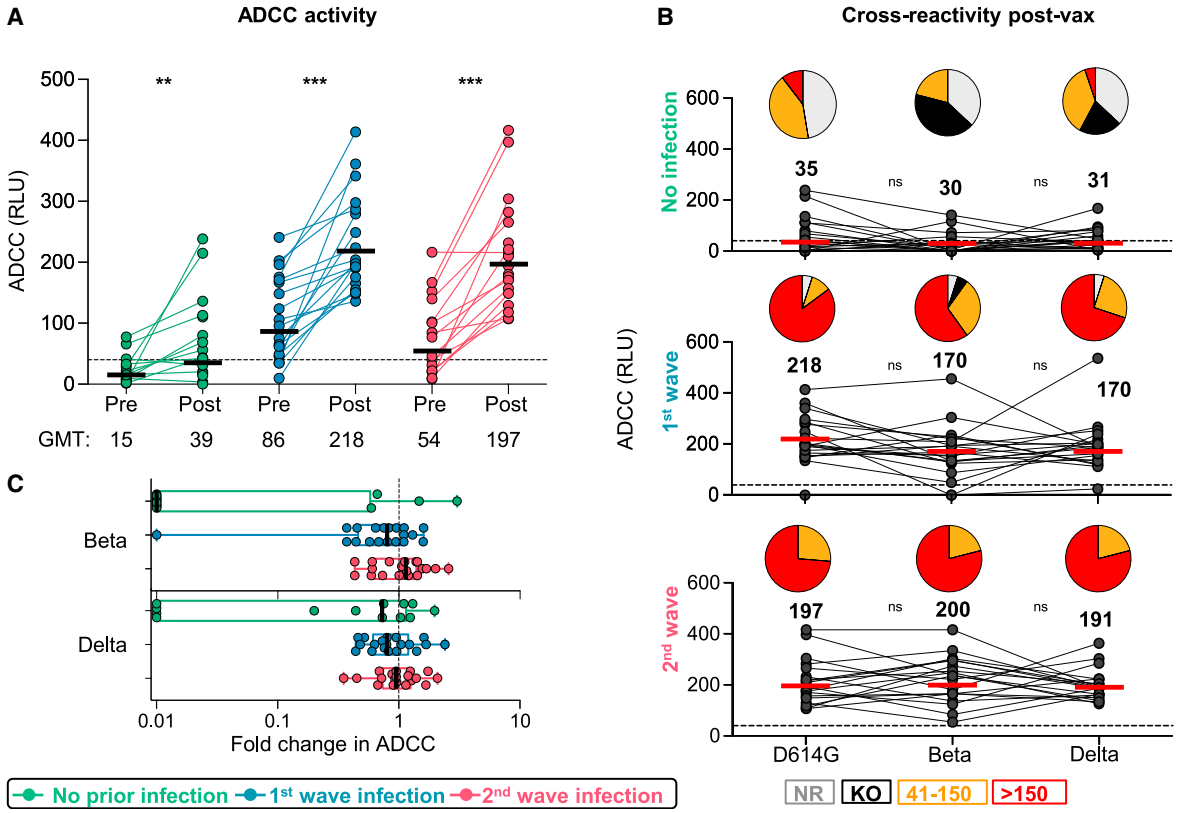

Figure 3. ADCC responses to Ad26.COV2.S vaccination

(A) ADCC activity represented as relative light units (RLU).

(B) Cross-reactive ADCC activity 28 days post-vaccination against D614G, Beta, and Delta. Pie charts show the proportion of vaccine non-responders (NR; gray), knockout of Beta/Delta neutralization (KO; black), or detectable ADCC activity (41–150, orange; >150, red). Statistical analyses were performed with the Friedman test between groups and the Wilcoxon test for pre- and post-vaccine time points or D614G in comparison with Beta/Delta responses. *$p < 0.05$, **$p < 0.01$, ***$p < 0.001$.

(C) Fold change of post-vaccination D614G ADCC levels relative to those of the Beta/Delta variants. The vertical bars indicate median fold difference and error bars the IQR.

against both Beta and Delta, consistent with previous studies (Liu et al., 2021). However, although Beta infection resulted in the preserved neutralization of D614G, we, like others (Liu et al., 2021), noted significant loss of activity against Delta. Therefore, although all participants were exposed to the same vaccine, the genotype of the infecting virus determined the specificity of the responses, prior to vaccine boosting. These findings have important implications for vaccine design, because the sequence of VOC spikes in second-generation vaccines could impact the repertoire of vaccine-induced antibodies.

Fc effector functions are important in vaccine-elicited protection against many viruses (Richardson and Moore, 2021). Reduced SARS-CoV-2 severity/mortality correlates with Fc effector activity (Zohar et al., 2020), and monoclonal antibodies could require Fc function for optimal protection (Winkler et al., 2021; Schäfer et al., 2021). We show that Ad26.COV.2 vaccination in SARS-CoV-2-naive HCWs elicits significant ADCC responses, consistent with previous data (Stephenson et al., 2021). In addition, prior infection significantly enhanced vaccine-elicited ADCC responses, independent of time post-infection, as for the BNT162b2 vaccine (Geers et al., 2021; Tauzin et al., 2021). Finally, unlike neutralizing antibodies, ADCC activity through vaccination alone, or boosted by prior infection, was cross-reactive for Beta and Delta. This is consistent with previous findings and suggests that ADCC-mediating antibodies target regions of the spike beyond the major neutralization epitopes (Alter et al., 2021).

SARS-CoV-2-specific T cells play a key role in modulating coronavirus disease 2019 (COVID-19) disease severity (Rydyznski Moderbacher et al., 2020) and provide protective immunity in the context of low antibody titers (McMahan et al., 2021). We show that robust spike-specific CD4 and CD8 memory T cell responses were induced by AD26.COV2.S vaccination, consistent with the findings of Alter et al. (2021). The magnitude of vaccine-induced T cell responses was similar to that of convalescent responses. The effect of prior infection was distinct from the antibody response, with CD4 responses in the infection naive group induced to a similar magnitude as the first-wave group, and existing CD4 T cells were only moderately boosted, if at all, in the second-wave group. There was an increase in the magnitude and proportion of CD8 responses to spike induced *de novo* after vaccination, in comparison with that seen in infection, similar for the three study groups. Four participants in the infection naive group displayed spike-specific CD8 T cells prior to vaccination, as described elsewhere, likely through exposure to endemic

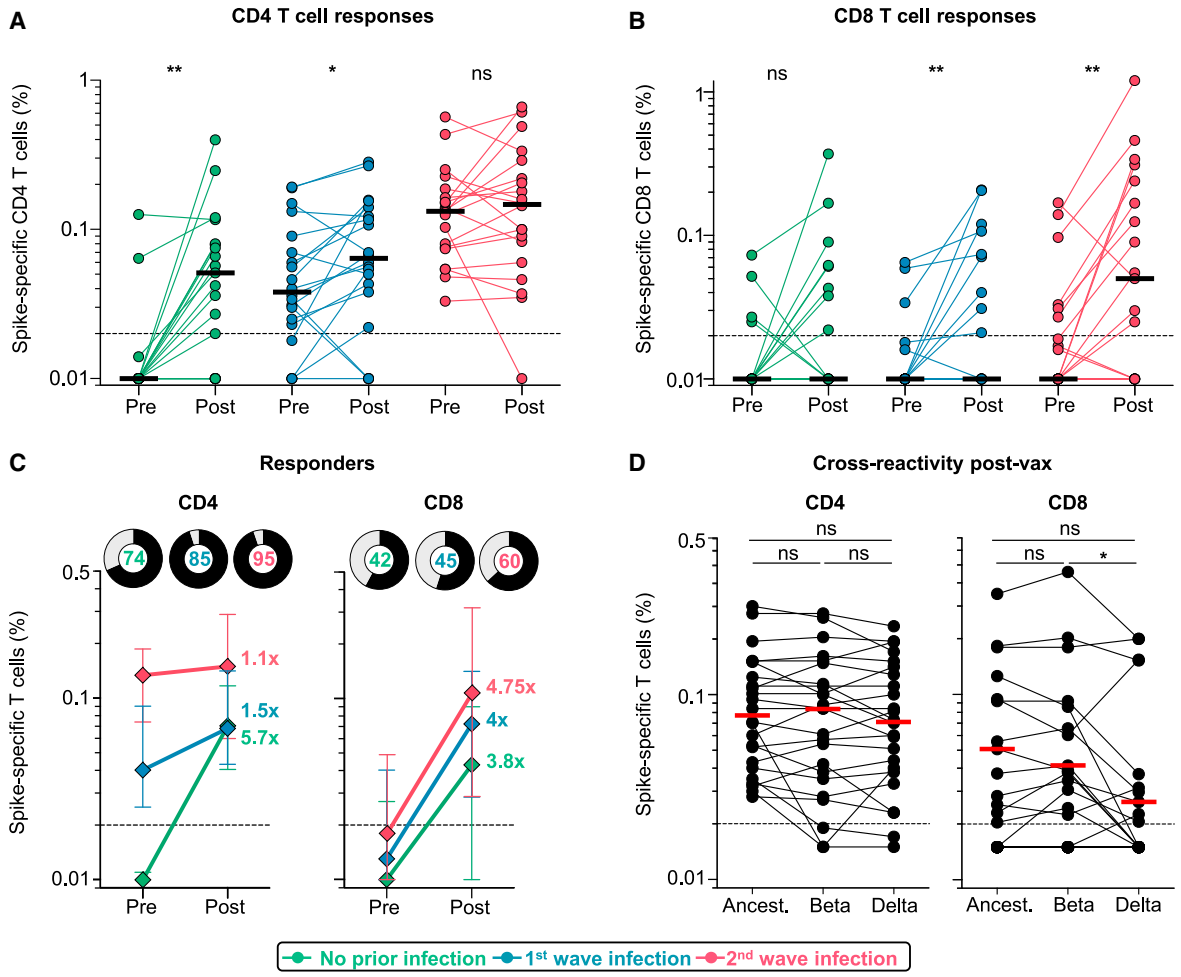

Figure 4. T cell responses to Ad26.COV2.S vaccination

(A and B) Frequency of total cytokine-producing spike-specific CD4 T cells (A) and CD8 T cells (B) in those with no prior infection (green, n = 19), infection in the first wave (blue, n = 20), and infection in the second wave (red, n = 19), in PBMCs stimulated with peptides based on Wuhan spike.

(C) Median fold change of CD4 and CD8 T cell frequencies after vaccination in responders. Error bars indicate IQR. Pie charts show responders (black) and non-responders (gray), with the percentage of responders indicated.

(D) Cross-reactivity of T cell responses post-vaccination (n = 24) after peptide stimulation with spike from the ancestral strain, Beta, or Delta is shown. Horizontal bars indicate medians. The dotted line indicates the threshold for positivity and values are background subtracted. Statistical analyses were performed with the Wilcoxon test. *p < 0.05, **p < 0.01.

human coronaviruses (Braun et al., 2020; Grifoni et al., 2020; Mateus et al., 2020). Of note, most CD8 responses declined after vaccination, suggesting a lack of cognate cross-reactivity.

Vaccination induced T cells that largely cross-recognized peptides based on Beta and Delta spike, suggesting that most vaccinees target conserved epitopes in spike, as previously described (Reynolds et al., 2021; Riou et al., 2021; Gallagher et al., 2021; Geers et al., 2021; Tarke et al., 2021). However, a third of vaccinees showed reduced CD8 recognition of Delta, which harbors the L452R mutation that confers resistance to human leukocyte antigen (HLA)-A*24:02 recognition (Motozono et al., 2021). Thus, reduced CD8 recognition of Delta might be attributed to the HLA repertoire of individuals.

Overall, we show a dramatic effect of recent or distant infection on the magnitude and breadth of neutralizing responses and ADCC. Ad26.COV2.S vaccination alone drives continued maturation of B cell responses, conferring enhanced neutralization of variants and durability (Barouch et al., 2021). It is still unknown whether prior infection will enhance maturation of neutralizing antibodies and extend durability further. T cell responses, though more modestly impacted by prior infection, were robust and largely cross-reactive. This suggests that an infection "prime" boosts Ad26.COV2.S immunogenicity and, in areas of high seroprevalence, could positively impact the effectiveness of this single-dose vaccine. Most significantly, we show that breadth of neutralization after vaccination is dictated by the infecting variant, with important implications for adapted vaccines based on VOCs.

Limitations of the study

This study focused on variant-specific responses post-vaccination, and we did not fully assess neutralizing breadth prior to vaccination. However, several studies have now characterized

the neutralizing activity against VOCs, including Delta, which now dominates globally and shows approximately 4- to 6-fold reduced sensitivity to convalescent plasma, in comparison with D614G (Edara et al., 2021; Liu et al., 2021; Planas et al., 2021). Furthermore, whether vectored vaccines predominantly elicit or boost pre-existing receptor binding domain responses, like mRNA vaccines (Stamatatos et al., 2021), remains to be defined. Finally, further analyses to identify the HLA alleles associated with reduced CD8 T cell cross-reactivity to Delta, and confirmation of the mutation(s) that are responsible for epitope loss, would shed light on the significance of cellular immune evasion by Delta.

STAR★METHODS

Detailed methods are provided in the online version of this paper and include the following:

- KEY RESOURCES TABLE
- RESOURCE AVAILABILITY
  - Lead contact
  - Materials availability
  - Data and code availability
- EXPERIMENTAL MODEL AND SUBJECT DETAILS
  - Human subjects
  - Cell lines
- METHOD DETAILS
  - SARS-CoV-2 spike WGS and phylogenetic analysis
  - Roche serology
  - Isolation of PBMC
  - SARS-CoV-2 antigens
  - SARS-CoV-2 spike ELISA
  - Pseudovirus neutralization assay
  - ADCC assay
  - Cell stimulation and flow cytometry staining
- QUANTIFICATION AND STATISTICAL ANALYSIS

SUPPLEMENTAL INFORMATION

Supplemental information can be found online at https://doi.org/10.1016/j.chom.2021.10.003.

ACKNOWLEDGMENTS

We thank the study participants and the clinical staff and personnel at Groote Schuur Hospital, Cape Town for their dedication. We thank F. Ayres, D. Mhlanga, B. Oosthuysen, and B. Lambson for production of protein and pseudoviruses. The parental soluble spike was provided by J. McLellan. The parental pseudovirus plasmids were kindly provided by Drs E. Landais and D. Sok. We thank the Variant Consortium of South African scientists. The graphical abstract was created with BioRender.com. This research was supported by the South African Medical Research Council, with funds received from the South African Department of Science and Innovation (DSI), including grants 96825, SHIPNCD 76756, and DST/CON 0250/2012. This work was supported by the Poliomyelitis Research Foundation (21/65) and the Wellcome Centre for Infectious Diseases Research in Africa (CIDRI-Africa), which is supported by core funding from the Wellcome Trust (203135/Z/16/Z and 222754). Funding support was received from NIH NIAID with the SARS-CoV-2 Assessment of Viral Evolution program and contract no. 75N9301900065 to A.S. and D.W. P.L.M. and S.I.R. are supported by the South African Research Chairs Initiative of DSI and the National Research Foundation (NRF; no. 98341). S.I.R. is a L'Oreal/UNESCO Women in Science South Africa Young Talents awardee. W.A.B. and C.R. are supported by the EDCTP2 program of the European Union's Horizon 2020 program (TMA2017SF-1951-TB-SPEC and TMA2016SF-1535-CaTCH-22). N.A.B.N. acknowledges funding from the SA-MRC, MRC UK, NRF, and the Lily and Ernst Hausmann Trust. M.N. is supported by the Wellcome Trust (207511/Z/17/Z) and by NIHR Biomedical Research Funding to University College London Hospitals. For the purposes of open access, the authors have applied a CC BY public copyright license to any author-accepted version arising from this submission.

AUTHOR CONTRIBUTIONS

W.A.B., P.L.M., and N.A.B.N. designed the study. W.A.B. and P.L.M. analyzed the data and wrote the manuscript. R.K., S.I.R., and T.M.G. generated and analyzed the data and wrote the manuscript. S.I.R., T.M.G., T.H., N.P.M., Z.M., and T.M. performed antibody assays. R.K., M.B.T., N.B., R.B., and A.N. performed T cell assays. M.M., S.S., and L.R.C. managed the HCW cohort and contributed clinical samples. A.O. and T.B. characterized the serological profiles. N.Y.H. contributed samples, and A.G., D.W., and A.S. provided variant peptide pools. D.D., A.I., and C.W. performed viral sequencing. H.M. and J.B. contributed to cohort characterization. C.R. contributed to data analysis. A.G., N.G., L.G.B., and G.G. established and led the Sisonke vaccine study. N.A.B.N., J.M., and M.N. established and led the HCW cohort. All authors reviewed and edited the manuscript.

DECLARATION OF INTERESTS

A.S. is a consultant for Gritstone, Flow Pharma, CellCarta, Arcturus, Oxford Immunotech, and Avalia. All of the other authors declare no competing interests. LJI has filed for patent protection for various aspects of vaccine design and identification of specific epitopes.

Received: July 23, 2021
Revised: September 10, 2021
Accepted: October 7, 2021
Published: October 13, 2021

REFERENCES

Alter, G., Yu, J., Liu, J., Chandrashekar, A., Borducchi, E.N., Tostanoski, L.H., McMahan, K., Jacob-Dolan, C., Martinez, D.R., Chang, A., et al. (2021). Immunogenicity of Ad26.COV2.S vaccine against SARS-CoV-2 variants in humans. Nature *596*, 268–272. https://doi.org/10.1038/s41586-021-03681-2.

Barouch, D.H., Stephenson, K.E., Sadoff, J., Yu, J., Chang, A., Gebre, M., McMahan, K., Liu, J., Chandrashekar, A., Patel, S., et al. (2021). Durable Humoral and Cellular Immune Responses 8 Months after Ad26.COV2.S Vaccination. N. Engl. J. Med. *385*, 951–953. https://doi.org/10.1056/NEJMc2108829.

Braun, J., Loyal, L., Frentsch, M., Wendisch, D., Georg, P., Kurth, F., Hippenstiel, S., Dingeldey, M., Kruse, B., Fauchere, F., et al. (2020). SARS-CoV-2-reactive T cells in healthy donors and patients with COVID-19. Nature *587*, 270–274. https://doi.org/10.1038/s41586-020-2598-9.

Cele, S., Gazy, I., Jackson, L., Hwa, S.H., Tegally, H., Lustig, G., Giandhari, J., Pillay, S., Wilkinson, E., Naidoo, Y., et al.; Network for Genomic Surveillance in South Africa; COMMIT-KZN Team (2021). Escape of SARS-CoV-2 501Y.V2 from neutralization by convalescent plasma. Nature *593*, 142–146. https://doi.org/10.1038/s41586-021-03471-w.

Cleemput, S., Dumon, W., Fonseca, V., Abdool Karim, W., Giovanetti, M., Alcantara, L.C., Deforche, K., and de Oliveira, T. (2020). Genome Detective Coronavirus Typing Tool for rapid identification and characterization of novel coronavirus genomes. Bioinformatics *36*, 3552–3555. https://doi.org/10.1093/bioinformatics/btaa145.

Edara, V.V., Pinsky, B.A., Suthar, M.S., Lai, L., Davis-Gardner, M.E., Floyd, K., Flowers, M.W., Wrammert, J., Hussaini, L., Ciric, C.R., et al. (2021). Infection and Vaccine-Induced Neutralizing-Antibody Responses to the SARS-CoV-2 B.1.617 Variants. N. Engl. J. Med. *385*, 664–666. https://doi.org/10.1056/nejmc2107799.

Gallagher, K.M.E., Leick, M.B., Larson, R.C., Berger, T.R., Katsis, K., Yam, J.Y., Brini, G., Grauwet, K., and Maus, M.V.; MGH COVID-19 Collection & Processing Team (2021). SARS -CoV-2 T-cell immunity to variants of concern following vaccination. bioRxiv. https://doi.org/10.1101/2021.05.03.442455.

Geers, D., Shamier, M.C., Bogers, S., den Hartog, G., Gommers, L., Nieuwkoop, N.N., Schmitz, K.S., Rijsbergen, L.C., van Osch, J.A.T., Dijkhuizen, E., et al. (2021). SARS-CoV-2 variants of concern partially escape humoral but not T-cell responses in COVID-19 convalescent donors and vaccinees. Sci. Immunol. *6*, eabj1750. https://doi.org/10.1126/sciimmunol.abj1750.

Grifoni, A., Weiskopf, D., Ramirez, S.I., Mateus, J., Dan, J.M., Moderbacher, C.R., Rawlings, S.A., Sutherland, A., Premkumar, L., Jadi, R.S., et al. (2020). Targets of T Cell Responses to SARS-CoV-2 Coronavirus in Humans with COVID-19 Disease and Unexposed Individuals. Cell *181*, 1489–1501.e15. https://doi.org/10.1016/j.cell.2020.05.015.

Hadfield, J., Megill, C., Bell, S.M., Huddleston, J., Potter, B., Callender, C., Sagulenko, P., Bedford, T., and Neher, R.A. (2018). Nextstrain: real-time tracking of pathogen evolution. Bioinformatics *34*, 4121–4123. https://doi.org/10.1093/bioinformatics/bty407.

Havervall, S., Marking, U., Greilert-Norin, N., Ng, H., Gordon, M., Salomonsson, A.C., Hellström, C., Pin, E., Blom, K., Mangsbo, S., et al. (2021). Antibody responses after a single dose of ChAdOx1 nCoV-19 vaccine in healthcare workers previously infected with SARS-CoV-2. EBioMedicine *70*, 103523. https://doi.org/10.1101/2021.05.08.21256866.

Hsiao, M., Davies, M., and Kalk, E. (2020). SARS-CoV-2 seroprevalence in the Cape Town Metropolitan sub-districts after the peak of infections. NICD COVID-19 Special Public Health Surveill Bull *18*, 1–9.

Hsieh, C.-L., Goldsmith, J.A., Schaub, J.M., DiVenere, A.M., Kuo, H.-C., Javanmardi, K., Le, K.C., Wrapp, D., Lee, A.G., Liu, Y., et al. (2020). Structure-based design of prefusion-stabilized SARS-CoV-2 spikes. Science *369*, 1501–1505. https://doi.org/10.1126/science.abd0826.

Liu, C., Ginn, H.M., Dejnirattisai, W., Supasa, P., Wang, B., Tuekprakhon, A., Nutalai, R., Zhou, D., Mentzer, A.J., Zhao, Y., et al. (2021). Reduced neutralization of SARS-CoV-2 B.1.617 by vaccine and convalescent serum. Cell *184*, 4220–4236.e13. https://doi.org/10.1016/j.cell.2021.06.020.

Manisty, C., Otter, A.D., Treibel, T.A., McKnight, Á., Altmann, D.M., Brooks, T., Noursadeghi, M., Boyton, R.J., Semper, A., and Moon, J.C. (2021). Antibody response to first BNT162b2 dose in previously SARS-CoV-2-infected individuals. Lancet *397*, 1057–1058. https://doi.org/10.1016/S0140-6736(21)00501-8.

Mateus, J., Grifoni, A., Tarke, A., Sidney, J., Ramirez, S.I., Dan, J.M., Burger, Z.C., Rawlings, S.A., Smith, D.M., Phillips, E., et al. (2020). Selective and cross-reactive SARS-CoV-2 T cell epitopes in unexposed humans. Science *370*, 89–94. https://doi.org/10.1126/science.abd3871.

McMahan, K., Yu, J., Mercado, N.B., Loos, C., Tostanoski, L.H., Chandrashekar, A., Liu, J., Peter, L., Atyeo, C., Zhu, A., et al. (2021). Correlates of protection against SARS-CoV-2 in rhesus macaques. Nature *590*, 630–634. https://doi.org/10.1038/s41586-020-03041-6.

Moore, P., Moyo-Gwete, T., Hermanus, T., Kgagudi, P., Ayres, F., Makhado, Z., Sadoff, J., Le Gars, M., van Roey, G., Crowther, C., et al. (2021). Neutralizing antibodies elicited by the Ad26.COV2.S COVID-19 vaccine show reduced activity against 501Y.V2 (B. 1.351), despite protection against severe disease by this variant. bioRxiv. https://doi.org/10.1101/2021.06.09.447722.

Motozono, C., Toyoda, M., Zahradnik, J., Saito, A., Nasser, H., Tan, T.S., Ngare, I., Kimura, I., Uriu, K., Kosugi, Y., et al.; Genotype to Phenotype Japan (G2P-Japan) Consortium (2021). SARS-CoV-2 spike L452R variant evades cellular immunity and increases infectivity. Cell Host Microbe *29*, 1124–1136.e11. https://doi.org/10.1016/j.chom.2021.06.006.

Moyo-Gwete, T., Madzivhandila, M., Makhado, Z., Ayres, F., Mhlanga, D., Oosthuysen, B., Lambson, B.E., Kgagudi, P., Tegally, H., Iranzadeh, A., et al. (2021). Cross-Reactive Neutralizing Antibody Responses Elicited by SARS-CoV-2 501Y.V2 (B.1.351). N. Engl. J. Med. *384*, 2161–2163. https://doi.org/10.1056/NEJMc2104192.

Mutevedzi, P.C., Kawonga, M., Kwatra, G., Moultrie, A., Baillie, V.L., Mabhena, N., Mathibe, M.N., Rafuma, M.M., Maposa, I., and Abbott, G. (2021). Population Based SARS-CoV-2 Sero-Epidemiological Survey and Estimated Infection Incidence and Fatality Risk in Gauteng Province, South Africa. https://ssrn.com/abstract=3855442.

Planas, D., Veyer, D., Baidaliuk, A., Staropoli, I., Guivel-Benhassine, F., Rajah, M.M., Planchais, C., Porrot, F., Robillard, N., Puech, J., et al. (2021). Reduced sensitivity of SARS-CoV-2 variant Delta to antibody neutralization. Nature *596*, 276–280. https://doi.org/10.1038/s41586-021-03777-9.

Reynolds, C.J., Pade, C., Gibbons, J.M., Butler, D.K., Otter, A.D., Menacho, K., Fontana, M., Smit, A., Sackville-West, J.E., Cutino-Moguel, T., et al.; UK COVIDsortium Immune Correlates Network; UK COVIDsortium Investigators (2021). Prior SARS-CoV-2 infection rescues B and T cell responses to variants after first vaccine dose. Science *372*, 1418–1423. https://doi.org/10.1126/science.abh1282.

Richardson, S.I., and Moore, P.L. (2021). Targeting Fc effector function in vaccine design. Expert Opin. Ther. Targets *25*, 467–477. https://doi.org/10.1080/14728222.2021.1907343.

Riou, C., Keeton, R., Moyo-Gwete, T., Hermanus, T., Kgagudi, P., Baguma, R., Tegally, H., Doolabh, D., Iranzadeh, A., Tyers, L., et al. (2021). Loss of recognition of SARS-CoV-2 B.1.351 variant spike epitopes but overall preservation of T cell immunity. medRxiv. https://doi.org/10.1101/2021.06.03.21258307.

Rydyznski Moderbacher, C., Ramirez, S.I., Dan, J.M., Grifoni, A., Hastie, K.M., Weiskopf, D., Belanger, S., Abbott, R.K., Kim, C., Choi, J., et al. (2020). Antigen-Specific Adaptive Immunity to SARS-CoV-2 in Acute COVID-19 and Associations with Age and Disease Severity. Cell *183*, 996–1012.e19. https://doi.org/10.1016/j.cell.2020.09.038.

Saadat, S., Rikhtegaran Tehrani, Z., Logue, J., Newman, M., Frieman, M.B., Harris, A.D., and Sajadi, M.M. (2021). Binding and neutralization antibody titers after a single vaccine dose in health care workers previously infected with SARS-CoV-2. JAMA *325*, 1467–1469. https://doi.org/10.1001/jama.2021.3341.

Sadoff, J., Gray, G., Vandebosch, A., Cárdenas, V., Shukarev, G., Grinsztejn, B., Goepfert, P.A., Truyers, C., Fennema, H., Spiessens, B., et al.; ENSEMBLE Study Group (2021). Safety and efficacy of single-dose Ad26. COV2. S vaccine against Covid-19. N. Engl. J. Med. *384*, 2187–2201. https://doi.org/10.1056/NEJMoa2101544.

Schäfer, A., Muecksch, F., Lorenzi, J.C.C., Leist, S.R., Cipolla, M., Bournazos, S., Schmidt, F., Maison, R.M., Gazumyan, A., Martinez, D.R., et al. (2021). Antibody potency, effector function, and combinations in protection and therapy for SARS-CoV-2 infection in vivo. J. Exp. Med. *218*, e20201993. https://doi.org/10.1084/jem.20201993.

Stamatatos, L., Czartoski, J., Wan, Y.H., Homad, L.J., Rubin, V., Glantz, H., Neradilek, M., Seydoux, E., Jennewein, M.F., MacCamy, A.J., et al. (2021). mRNA vaccination boosts cross-variant neutralizing antibodies elicited by SARS-CoV-2 infection. Science, eabg9175. https://doi.org/10.1126/science.abg9175.

Stephenson, K.E., Le Gars, M., Sadoff, J., de Groot, A.M., Heerwegh, D., Truyers, C., Atyeo, C., Loos, C., Chandrashekar, A., McMahan, K., et al. (2021). Immunogenicity of the Ad26.COV2.S Vaccine for COVID-19. JAMA *325*, 1535–1544. https://doi.org/10.1001/jama.2021.3645.

Sykes, W., Mhlanga, L., Swanevelder, R., Glatt, T.N., Grebe, E., Coleman, C., Pieterson, N., Cable, R., Welte, A., van den Berg, K., and Vermeulen, M. (2021). Prevalence of anti-SARS-CoV-2 antibodies among blood donors in Northern Cape, KwaZulu-Natal, Eastern Cape, and Free State provinces of South Africa in January 2021. Res Sq. rs.3.rs-233375. https://doi.org/10.21203/rs.3.rs-233375/v1.

Takuva, S., Takalani, A., Garrett, N., Goga, A., Peter, J., Louw, V., Opie, J., Jacobson, B., Sanne, I., Gail-Bekker, L., and Gray, G. (2021). Thromboembolic Events in the South African Ad26.COV2.S Vaccine Study. N. Engl. J. Med. *385*, 570–571. https://doi.org/10.1056/NEJMc2107920.

Tarke, A., Sidney, J., Methot, N., Yu, E.D., Zhang, Y., Dan, J.M., Goodwin, B., Rubiro, P., Sutherland, A., Wang, E., et al. (2021). Impact of SARS-CoV-2 variants on the total $CD4^+$ and $CD8^+$ T cell reactivity in infected or vaccinated

individuals. Cell Rep Med *2*, 100355. https://doi.org/10.1016/j.xcrm.2021.100355.

Tauzin, A., Nayrac, M., Benlarbi, M., Gong, S.Y., Gasser, R., Beaudoin-Bussières, G., Brassard, N., Laumaea, A., Vézina, D., Prévost, J., et al. (2021). A single dose of the SARS-CoV-2 vaccine BNT162b2 elicits Fc-mediated antibody effector functions and T cell responses. Cell Host Microbe *29*, 1137–1150.e6. https://doi.org/10.1016/j.chom.2021.06.001.

Tegally, H., Wilkinson, E., Giovanetti, M., Iranzadeh, A., Fonseca, V., Giandhari, J., Doolabh, D., Pillay, S., San, E.J., Msomi, N., et al. (2021). Detection of a SARS-CoV-2 variant of concern in South Africa. Nature *592*, 438–443. https://doi.org/10.1038/s41586-021-03402-9.

Vanshylla, K., Di Cristanziano, V., Kleipass, F., Dewald, F., Schommers, P., Gieselmann, L., Gruell, H., Schlotz, M., Ercanoglu, M.S., Stumpf, R., et al. (2021). Kinetics and correlates of the neutralizing antibody response to SARS-CoV-2 infection in humans. Cell Host Microbe *29*, 917–929.e4. https://doi.org/10.1016/j.chom.2021.04.015.

Wang, P., Nair, M.S., Liu, L., Iketani, S., Luo, Y., Guo, Y., Wang, M., Yu, J., Zhang, B., Kwong, P.D., et al. (2021a). Antibody resistance of SARS-CoV-2 variants B.1.351 and B.1.1.7. Nature *593*, 130–135. https://doi.org/10.1038/s41586-021-03398-2.

Wang, Z., Muecksch, F., Schaefer-Babajew, D., Finkin, S., Viant, C., Gaebler, C., Hoffmann, H.-H., Barnes, C.O., Cipolla, M., Ramos, V., et al. (2021b). Naturally enhanced neutralizing breadth against SARS-CoV-2 one year after infection. Nature *595*, 426–431. https://doi.org/10.1038/s41586-021-03696-9.

Wibmer, C.K., Ayres, F., Hermanus, T., Madzivhandila, M., Kgagudi, P., Oosthuysen, B., Lambson, B.E., de Oliveira, T., Vermeulen, M., van der Berg, K., et al. (2021). SARS-CoV-2 501Y.V2 escapes neutralization by South African COVID-19 donor plasma. Nat. Med. *27*, 622–625. https://doi.org/10.1038/s41591-021-01285-x.

Winkler, E.S., Gilchuk, P., Yu, J., Bailey, A.L., Chen, R.E., Chong, Z., Zost, S.J., Jang, H., Huang, Y., Allen, J.D., et al. (2021). Human neutralizing antibodies against SARS-CoV-2 require intact Fc effector functions for optimal therapeutic protection. Cell *184*, 1804–1820.e16. https://doi.org/10.1016/j.cell.2021.02.026.

Zohar, T., Loos, C., Fischinger, S., Atyeo, C., Wang, C., Slein, M.D., Burke, J., Yu, J., Feldman, J., Hauser, B.M., et al. (2020). Compromised humoral functional evolution tracks with SARS-CoV-2 mortality. Cell *183*, 1508–1519.e12. https://doi.org/10.1016/j.cell.2020.10.052.

STAR★METHODS

KEY RESOURCES TABLE

REAGENT or RESOURCE	SOURCE	IDENTIFIER
Antibodies		
purified NA/LE mouse anti-human CD28 (clone 28.2)	BD PharMingen	Cat# 555725; RRID: AB_2130052
purified NA/LE mouse anti-human CD49d (clone L25)	BD PharMingen	Cat# 555501; RRID: AB_396068
LIVE/DEAD™ Fixable VIVID Stain	Invitrogen	Cat# L34955
CD14 Pac Blue (clone TuK4)	Invitrogen Thermofisher Scientific	Cat# MHCD1428; RRID: AB_10373537
CD19 Pac Blue (clone SJ25-C1)	Invitrogen Thermofisher Scientific	Cat# MHCD1928; RRID: AB_10373689
CD4 PERCP-Cy5.5 (clone L200)	BD Biosciences	Cat# 552838; RRID: AB_394488
CD8 BV510 (clone RPA-8)	Biolegend	Cat# 301048; RRID: AB_2561942
PD-1 BV711 (clone EH12.2H7)	Biolegend	Cat# 329928; RRID: AB_11218612
CD27 PE-Cy5 (clone 1A4)	Beckman Coulter	Cat# 6607107; RRID: AB_10641617)
CD45RA BV570 (clone HI100)	Biolegend	Cat# 304132; RRID: AB_2563813
CD3 BV650 (clone OKT3)	Biolegend	Cat# 317324; RRID: AB_2563352
IFN-g Alexo 700 (clone B27)	BD Biosciences	Cat# 557995; RRID: AB_396977
TNF BV786 (clone Mab11)	Biolegend	Cat# 502948; RRID: AB_2565858
IL-2 APC (clone MQ1-17H12)	Biolegend	Cat# 500310; RRID: AB_315097
CR3022	Genscript (https://www.genscript.com)	N/A
BD23	Dr Nicole Doria-Rose, VRC, USA	N/A
P2B-2F6	Dr Nicole Doria-Rose, VRC, USA	N/A
anti-IgG APC (clone QA19A42)	Biolegend	Cat#366905 RRID: AB_2888847
Palivizumab	Medimmune	Synagis; RRID: AB_2459638
Bacterial and virus strains		
SARS-CoV-2 pseudoviruses for ancestral, Beta and Delta	Wibmer et al., 2021; This paper	N/A
Biological samples		
Convalescent health care worker blood samples	Groote Schuur Hospital	https://www.gsh.co.za
Chemicals, peptides, and recombinant proteins		
PepTivator® SARS-CoV-2 Prot_S	Miltenyi Biotech	Cat #130-126-701
PepTivator® SARS-CoV-2 Prot_S1	Miltenyi Biotech	Cat# 130-127-048
SARS-CoV-2 Original Wuhan, Beta and Delta spike synthetic peptides	TC Peptide Lab	https://tcpeptidelab.com
SARS-CoV-2 original and Beta variant spike proteins	Original: Hsieh et al., 2020; Beta: Moyo-Gwete et al., 2021	N/A
Critical commercial assays		
Superscript IV Reverse Transcriptase	Life Technologies, Carlsbad, CA	Cat # 18090200
Qubit dsDNA High Sensitivity assay	Life Technologies Carlsbad, CA	Cat # Q32854
AMPure XP magnetic beads	Beckman Coulter	Cat # A63881
Illumina® DNA Prep kit	Illumina, San Diego	Cat # 20018705
Nextera™ DNA CD Indexes (96 Indexes, 96 Samples)	Illumina, San Diego	Cat # 20018708
Elecsys anti-SARS-CoV-2 Spike immunoassay	Roche Diagnostics	CAT# 09 289 275 190
Elecys anti-SARS-CoV-2 electrochemiluminescent immunoassay	Roche Diagnostics	CAT# 09 203 095 190
PEI-MAX 40,000	Polysciences	Cat # 24765-1
LIVE/DEAD™ Fixable VIVID Stain	Invitrogen	Cat # L34955

(*Continued on next page*)

Continued

REAGENT or RESOURCE	SOURCE	IDENTIFIER
Cytofix/Cyto perm buffer	BD Biosciences	Cat # 554722
CellFIX	BD Biosciences	Cat # 340181
QUANTI-Luc luciferase	Invivogen	Cat# rep-qlc2
Luciferase for neuts	Promega	Cat# PRE263B-C
Deposited data		
PID1054 SARS-CoV-2 Viral sequence	GISAID EpiCoV database	GISAID Accession # EPI_ISL_2621106
PID1127 SARS-CoV-2 Viral sequence	GISAID EpiCoV database	GISAID Accession # EPI_ISL_2621118
PID1128 SARS-CoV-2 Viral sequence	GISAID EpiCoV database	GSAID Accession # EPI_ISL_2621122
PID1134 SARS-CoV-2 Viral sequence	GISAID EpiCoV database	GISAID Accession # EPI_ISL_1534413
PID1169 SARS-CoV-2 Viral sequence	GISAID EpiCoV database	GISAID Accession # EPI_ISL_2621117
PID1319 SARS-CoV-2 Viral sequence	GISAID EpiCoV database	GISAID Accession # EPI_ISL_2621127
PID1337 SARS-CoV-2 Viral sequence	GISAID EpiCoV database	GISAID Accession # EPI_ISL_2621124
PID1399 SARS-CoV-2 Viral sequence	GISAID EpiCoV database	GISAID Accession # EPI_ISL_2621110
Ancestral (Wuhan)	www.ncbi.nlm.nih.gov	NC_045512.2
B.1.351 (Beta)	www.GISAID.org	EPI_ISL_660629
B.1.351 (Beta)	www.GISAID.org	EPI_ISL_736930
B.1.351 (Beta)	www.GISAID.org	EPI_ISL_736932
B.1.351 (Beta)	www.GISAID.org	EPI_ISL_736944
B.1.351 (Beta)	www.GISAID.org	EPI_ISL_736971
B.1.351 (Beta)	www.GISAID.org	EPI_ISL_736966
B.1.351 (Beta)	www.GISAID.org	EPI_ISL_736973
B.1.351 (Beta)	www.GISAID.org	EPI_ISL_825104
B.1.351 (Beta)	www.GISAID.org	EPI_ISL_825120
B.1.351 (Beta)	www.GISAID.org	EPI_ISL_825131
B.1.617.2 (Delta)	www.GISAID.org	EPI_ISL_2020950
Experimental models: Cell lines		
Human Embryonic Kidney (HEK) 293F	Dr Nicole Doria-Rose, VRC, USA	N/A
HEK293T-ACE2 cells	Dr Michael Farzan, Scripps, USA	N/A
Jurkat-Lucia™ NFAT-CD16 cells	Invivogen	Cat # jktl-nfat-cd16
Recombinant DNA		
Spike Hexapro plasmid	Original: Hsieh et al., 2020Beta: Moyo-Gwete et al., 2021	N/A
SARS-CoV-2 ancestral variant spike (D614G) plasmid	Wibmer et al., 2021	N/A
Beta spike (L18F, D80A, D215G, K417N, E484K, N501Y, D614G, A701V, 242-244 del) plasmid	Wibmer et al., 2021	N/A
Delta spike (T19R, R158G L452R, T478K, D614G, P681R, D950N, 156-157 del) plasmid	This paper	N/A
Firefly luciferase encoding lentivirus backbone plasmid	Dr Michael Farzan, Scripps	N/A
Software and algorithms		
Genome Detective 1.132	Genome Detective	https://www.genomedetective.com
Coronavirus Typing Tool	Cleemput et al., 2020	N/A
Geneious software	Biomatters Ltd	N/A
NextStrain	Hadfield et al., 2018	https://github.com/nextstrain/ncov
FACSDiva 9	BD Biosciences	https://www.bdbiosciences.com
FlowJo 10	FlowJo, LLC	https://www.flowjo.com
Graphpad Prism 9	Graphpad	https://graphpad.com
BioRender	BioRender	https://biorender.com

RESOURCE AVAILABILITY

Lead contact

Further information and requests for resources and reagents should be directed to and will be fulfilled by the lead contact, Wendy Burgers (wendy.burgers@uct.ac.za).

Materials availability

Materials will be made available by request to Wendy Burgers (wendy.burgers@uct.ac.za).

Data and code availability

The published article includes all data generated or analyzed during this study, and summarized in the accompanying tables, figures and supplemental information. The following sequences were deposited onto the GISAID EpiCov database (https://www.gisaid.org): PID1054 SARS-CoV-2 Viral sequence (GISAID Accession # EPI_ISL_2621106), PID1127 SARS-CoV-2 Viral sequence (GISAID Accession # EPI_ISL_2621118), PID1128 SARS-CoV-2 Viral sequence (GSAID Accession # EPI_ISL_2621122), PID1134 SARS-CoV-2 Viral sequence (GISAID Accession # EPI_ISL_1534413), PID1169 SARS-CoV-2 Viral sequence (GISAID Accession # EPI_ISL_2621117), PID1319 SARS-CoV-2 Viral sequence (GISAID Accession # EPI_ISL_2621127), PID1337 SARS-CoV-2 Viral sequence (GISAID Accession # EPI_ISL_2621124), PID1399 SARS-CoV-2 Viral sequence (GISAID Accession # EPI_ISL_2621110).

EXPERIMENTAL MODEL AND SUBJECT DETAILS

Human subjects

Participants were recruited from a longitudinal study of healthcare workers (HCW; n = 400) enrolled from Groote Schuur Hospital (Cape Town, Western Cape, South Africa). HCW in this cohort were recruited between July 2020 and January 2021, and vaccination with single dose Johnson and Johnson Ad26.COV2.S in the Sisonke Phase 3b trial took place between 17 February and 26 March 2021. Sixty participants were selected for inclusion in this study, based on the availability of PBMC and plasma prior to vaccination and approximately one month after vaccination, and who fell into one of three groups: (1) No evidence of previous SARS-CoV-2 infection by diagnostic PCR test or serial serology; (2) infection during the 'first wave' of the pandemic in South Africa, prior to 1 September 2020, with known date of laboratory (PCR)-confirmed SARS-CoV-2 infection; and (3) infection during the 'second wave', with known date of laboratory (PCR)-confirmed SARS-CoV-2 infection between 1 November 2020 and 31 January 2021. Full demographic and clinical characteristics of participants are summarized in Table S1. The study was approved by the University of Cape Town Human Research Ethics Committee (HREC 190/2020 and 209/2020) and the University of the Witwatersrand Human Research Ethics Committee (Medical) (no M210429). Written informed consent was obtained from all participants.

Cell lines

Human embryo kidney HEK293T cells were cultured at 37°C, 5% CO_2, in DMEM containing 10% heat-inactivated fetal bovine serum (GIBCO BRL Life Technologies) and supplemented with 50 μg/mL gentamicin (Sigma). Cells were disrupted at confluence with 0.25% trypsin in 1 mM EDTA (Sigma) every 48–72 h. HEK293T-ACE2 cells were maintained in the same way as HEK293T cells but were supplemented with 3 μg/mL puromycin for selection of stably transduced cells. Jurkat-Lucia NFAT-CD16 cells were maintained in IMDM media with 10% heat-inactivated fetal bovine serum (GIBCO, Gaithersburg, MD), 1% Penicillin Streptomycin (GIBCO, Gaithersburg, MD) and 10 μg/mL of Blasticidin and 100 μg/mL of Zeocin was added to the growth medium every other passage.

METHOD DETAILS

SARS-CoV-2 spike WGS and phylogenetic analysis

Whole genome sequencing (WGS) of SARS-CoV-2 was performed using nasopharyngeal swabs obtained from 19 of the hospitalized patients recruited during the second COVID-19 wave. Sequencing was performed as previously published (Moyo-Gwete et al., 2021). Briefly, cDNA was synthesized from RNA extracted from the nasopharyngeal swabs using the Superscript IV First Strand synthesis system (Life Technologies, Carlsbad, CA) and random hexamer primers. Whole genome amplification was then performed by multiplex PCR using the ARTIC V3 protocol (https://www.protocols.io/view/ncov-2019-sequencing-protocol-v3-locost-bh42j8ye). PCR products were purified with AMPure XP magnetic beads (Beckman Coulter, CA) and quantified using the Qubit dsDNA High Sensitivity assay on the Qubit 3.0 instrument (Life Technologies Carlsbad, CA). The Illumina® DNA Prep kit was used to prepare indexed paired end libraries of genomic DNA. Sequencing libraries were normalized to 4 nM, pooled, and denatured with 0.2 N sodium hydroxide. Libraries were sequenced on the Illumina MiSeq instrument (Illumina, San Diego, CA, USA). The quality control checks on raw sequence data and the genome assembly were performed using Genome Detective 1.132 (https://www.genomedetective.com) and the Coronavirus Typing Tool (Cleemput et al., 2020). The initial assembly obtained from Genome Detective was polished by aligning mapped reads to the references and filtering out low-quality mutations using bcftools 1.7-2 mpileup method. Mutations were confirmed visually with bam files using Geneious software (Biomatters Ltd, New Zealand). Phylogenetic clade classification of the genomes in this study consisted of analyzing them against a global reference dataset using a custom pipeline based on a local version of NextStrain (https://github.com/nextstrain/ncov) (Hadfield et al., 2018).

Roche serology

Serial serum samples were analyzed from longitudinal study visits from enrolment to post-vaccination (3-8 time points per participant) at Public Health England, Porton Down. The Elecsys anti-SARS-CoV-2 Spike and the Elecys anti-SARS-CoV-2 electrochemiluminescent immunoassays were performed (Roche Diagnostics, GmbH), which enable detection of total antibodies against the SARS-CoV-2 spike (S) receptor binding domain (RBD) and nucleocapsid (N) proteins, respectively. Samples were analyzed on a Cobas e801 instrument and a result $\geq$0.8 U/mL was considered positive in the S assay, and $\geq$1.0 U/mL positive in the N assay, according to the manufacturer's instructions.

Isolation of PBMC

Blood was collected in heparin tubes and processed within 3 h of collection. Peripheral blood mononuclear cells (PBMC) were isolated by density gradient sedimentation using Ficoll-Paque (Amersham Biosciences, Little Chalfont, UK) as per the manufacturer's instructions and cryopreserved in freezing media consisting of heat-inactivated fetal bovine serum (FBS, Thermofisher Scientific) containing 10% DMSO and stored in liquid nitrogen until use.

SARS-CoV-2 antigens

For serology assays, SARS-CoV-2 original and Beta variant spike proteins were expressed in Human Embryonic Kidney (HEK) 293F suspension cells by transfecting the cells with the spike plasmid. After incubating for six days at 37°C, 70% humidity and 10% CO_2, proteins were first purified using a nickel resin followed by size-exclusion chromatography. Relevant fractions were collected and frozen at −80°C until use.

For T cell assays, we used peptides covering the full length SARS-CoV-2 spike protein, by combining two commercially available peptide pools of 15-mer sequences with 11 amino acids (aa) overlap (PepTivator®, Miltenyi Biotech, Bergisch Gladbach, Germany). These peptides are based on the Wuhan-1 strain and cover the N-terminal S1 domain of SARS-CoV-2 from aa 1 to 692, as well as the majority of the C-terminal S2 domain. Pools were resuspended in distilled water at a concentration of 50 μg/mL and used at a final concentration of 1 μg/mL. To determine T cell responses to SARS-CoV-2 variants, peptides were synthesized that spanned the entire SARS-CoV-2 spike protein and corresponded to the ancestral Wuhan sequence (GenBank: MN908947) or the Beta (B.1.351; GISAID: EPI_ISL_736932, EPI_ISL_736944, EPI_ISL_736971, EPI_ISL_736966, EPI_ISL_736973, EPI_ISL_825104, EPI_ISL_825120,EPI_ISL_825131), as previously reported (Tarke et al., 2021) or to the Delta SARS-CoV-2 variants (B.1.617.2; GISAID: EPI_ISL_2020950). Peptides were 15-mers overlapping by 10 amino acids and were synthesized as crude material (TC Peptide Lab, San Diego, CA). All peptides were individually resuspended in dimethyl sulfoxide (DMSO) at a concentration of 10–20 mg/mL. Megapools for each antigen were created by pooling aliquots of these individual peptides in the respective SARS-CoV-2 spike sequences, followed by sequential lyophilization steps, and resuspension in DMSO at 1 mg/mL. Pools were used at a final concentration of 1 μg/mL with an equimolar DMSO concentration in the non-stimulated control.

SARS-CoV-2 spike ELISA

Two μg/mL of spike protein were used to coat 96-well, high-binding plates and incubated overnight at 4°C. The plates were incubated in a blocking buffer consisting of 5% skimmed milk powder, 0.05% Tween 20, 1x PBS. Plasma samples were diluted to 1:100 starting dilution in a blocking buffer and added to the plates. Secondary antibody was diluted to 1:3000 in blocking buffer and added to the plates followed by TMB substrate (Thermofisher Scientific). Upon stopping the reaction with 1 M H_2SO_4, absorbance was measured at a 450nm wavelength. In all instances, mAbs CR3022 and BD23 were used as positive controls and palivizumab was used as a negative control. All values were normalized with the CR3022 mAb.

Pseudovirus neutralization assay

SARS-CoV-2 pseudotyped lentiviruses were prepared by co-transfecting the HEK293T cell line with either the SARS-CoV-2 ancestral variant spike (D614G), the Beta spike (L18F, D80A, D215G, K417N, E484K, N501Y, D614G, A701V, 242-244 del) or the Delta spike (T19R, R158G L452R, T478K, D614G, P681R, D950N, 156-157 del) plasmids in conjunction with a firefly luciferase encoding lentivirus backbone plasmid. For the neutralization assay, heat-inactivated plasma samples from vaccine recipients were incubated with the SARS- CoV-2 pseudotyped virus for 1 h at 37°C, 5% CO_2. Subsequently, 1x104 HEK293T cells engineered to overexpress ACE-2 were added and incubated at 37°C, 5% CO_2 for 72 h upon which the luminescence of the luciferase gene was measured. CB6 was used as a positive control.

ADCC assay

The ability of plasma antibodies to cross-link FcγRIIIa (CD16) and spike expressing cells was measured as a proxy for antibody-dependent cellular cytotoxicity (ADCC). HEK293T cells were transfected with 5 μg of SARS-CoV-2 original variant spike (D614G), Beta or Delta spike plasmids using PEI-MAX 40,000 (Polysciences) and incubated for 2 days at 37°C. Expression of spike was confirmed by binding of CR3022 and P2B-2F6 and their detection by anti-IgG APC staining measured by flow cytometry. Subsequently, $1x10^5$ spike transfected cells per well were incubated with heat inactivated plasma (1:100 final dilution) or control mAbs (final concentration of 100 μg/mL) in RPMI 1640 media supplemented with 10% FBS 1% Pen/Strep (GIBCO, Gaithersburg, MD) for 1 h at 37°C. Jurkat-Lucia NFAT-CD16 cells (Invivogen) ($2x10^5$ cells/well) were added and incubated for 24 h at 37°C, 5% CO_2. Twenty μl of supernatant was then transferred to a white 96-well plate with 50 μL of reconstituted QUANTI-Luc secreted luciferase and read

immediately on a Victor 3 luminometer with 1 s integration time. Relative light units (RLU) of a no antibody control were subtracted as background. Palivizumab was used as a negative control, while CR3022 was used as a positive control, and P2B-2F6 to differentiate the Beta from the D614G variant. To induce the transgene 1x cell stimulation cocktail (Thermofisher Scientific, Oslo, Norway) and 2 μg/mL ionomycin in R10 was added as a positive control.

Cell stimulation and flow cytometry staining

Cryopreserved PBMC were thawed, washed and rested in RPMI 1640 containing 10% heat-inactivated FCS for 4 h prior to stimulation. PBMC were seeded in a 96-well V-bottom plate at ~2 × 10^6 PBMC per well and stimulated with SARS-CoV-2 spike peptide pools: full spike pool (Miltenyi), and ancestral and Beta mutated S1 and S2 pools (1 μg/mL). All stimulations were performed in the presence of Brefeldin A (10 μg/mL, Sigma-Aldrich, St Louis, MO, USA) and co-stimulatory antibodies against CD28 (clone 28.2) and CD49d (clone L25) (1 μg/mL each; BD Biosciences, San Jose, CA, USA). As a negative control, PBMC were incubated with co-stimulatory antibodies, Brefeldin A and an equimolar amount of DMSO.

After 16 h of stimulation, cells were washed, stained with LIVE/DEAD Fixable VIVID Stain (Invitrogen, Carlsbad, CA, USA) and subsequently surface stained with the following antibodies: CD14 Pac Blue (TuK4, Invitrogen Thermofisher Scientific), CD19 Pac Blue (SJ25-C1, Invitrogen Thermofisher Scientific), CD4 PERCP-Cy5.5 (L200, BD Biosciences, San Jose, CA, USA), CD8 BV510 (RPA-8, Biolegend, San Diego, CA, USA), PD-1 BV711 (EH12.2H7, Biolegend, San Diego, CA, USA), CD27 PE-Cy5 (1A4, Beckman Coulter), CD45RA BV570 (HI100, Biolegend, San Diego, CA, USA). Cells were then fixed and permeabilized using a Cytofix/Cyto perm buffer (BD Biosciences) and stained with CD3 BV650 (OKT3) IFN-g Alexo 700 (B27), TNF BV786 (Mab11) and IL-2 APC (MQ1-17H12) from Biolegend. Finally, cells were washed and fixed in CellFIX (BD Biosciences). Samples were acquired on a BD LSR-II flow cytometer and analyzed using FlowJo (v10, FlowJo LLC, Ashland, OR, USA). A median of 282 848 CD4 events (IQR:216 796 - 355 414) and 153 192 CD8 events (IQR 109 697 - 202 204) were acquired. Cells were gated on singlets, CD14-CD19-, live lymphocytes and memory cells (excluding naive CD27+ CD45RA+ population). Results are expressed as the frequency of CD4+ or CD8+ T cells expressing IFN-g, TNF-a or IL-2. Due to high TNF-a backgrounds, cells producing TNF-a alone were excluded from the analysis. Cytokine responses presented are background subtracted values (from the frequency of cytokine produced in unstimulated cells), and the threshold for a positive cytokine response was defined as > 0.02%.

QUANTIFICATION AND STATISTICAL ANALYSIS

Statistical analyses were performed in Prism (v9; GraphPad Software Inc, San Diego, CA, USA). Non-parametric tests were used for all comparisons. The Mann-Whitney, Friedman and Wilcoxon tests were used for unmatched and paired samples, respectively. All correlations reported are non-parametric Spearman's correlations. *P value*s less than 0.05 were considered statistically significant. Details of analysis performed for each experiment are described in the figure legends.

Cell Host & Microbe, Volume *29*

Supplemental information

Prior infection with SARS-CoV-2 boosts and broadens Ad26.COV2.S immunogenicity in a variant-dependent manner

Roanne Keeton, Simone I. Richardson, Thandeka Moyo-Gwete, Tandile Hermanus, Marius B. Tincho, Ntombi Benede, Nelia P. Manamela, Richard Baguma, Zanele Makhado, Amkele Ngomti, Thopisang Motlou, Mathilda Mennen, Lionel Chinhoyi, Sango Skelem, Hazel Maboreke, Deelan Doolabh, Arash Iranzadeh, Ashley D. Otter, Tim Brooks, Mahdad Noursadeghi, James C. Moon, Alba Grifoni, Daniela Weiskopf, Alessandro Sette, Jonathan Blackburn, Nei-Yuan Hsiao, Carolyn Williamson, Catherine Riou, Ameena Goga, Nigel Garrett, Linda-Gail Bekker, Glenda Gray, Ntobeko A.B. Ntusi, Penny L. Moore, and Wendy A. Burgers

Supplemental Table S1

Supplemental Table 1: Clinical and demographic details of study participants relating to Figure 1

	No previous infection (n=20)	First wave infection (n=20)	Second wave infection (n=20)
Demographic			
Age (years)[b]	48 [36-57]	35 [30-38]	36 [31-44]
Gender M:F (% Female)	3:17 (85%)	10:10 (50%)	5:15 (75%)
Ethnicity			
Black	1 (5%)	5 (25%)	7 (35%)
White	6 (30%)	9 (45%)	5 (25%)
Mixed	12 (60%)	6 (30%)	8 (40%)
Other	1 (5%)	0 (0%)	0 (0%)
Clinical			
SARS-CoV-2 PCR positivity	0%	100%	100%
Days after vaccination[b]	30 [27-33]	29 [28-33]	28 [28-37]
Days from PCR+ test to vaccination[b]	N/A[c]	232 [200-261]	73 [54-82]
Disease severity			
WHO Scale 2 (mild)[d]	N/A	20 (100%)	20 (100%)
Comorbidities			
Asthma	6 (30%)	2 (10%)	3 (15%)
Hypertension	3 (20%)	2 (10%)	2 (10%)
Obesity	2 (10%)	2 (10%)	1 (5%)
Diabetes mellitus	2 (10%)	2 (10%)	1 (5%)
HIV	0 (0%)	0 (0%)	0 (0%)
Other[e]	1 (5%)	1 (5%)	2 (5%)
None	8 (35%)	13 (65%)	12 (60%)
>1 comorbidity	1 (5%)	1 (5%)	1 (5%)

[a]Healthcare roles in the hospital included doctors (19), nurses (21), allied health professionals (11), administrative staff (5), cleaners (3), other (1); [b]median and interquartile range; [c]Not applicable; [d]World Health Organisation ordinal scale 2 (WHO Working Group on the Clinical Characterisation and Management of COVID-19 infection, 2020); [e]Other comorbidities not specified

Supplemental Figure S1

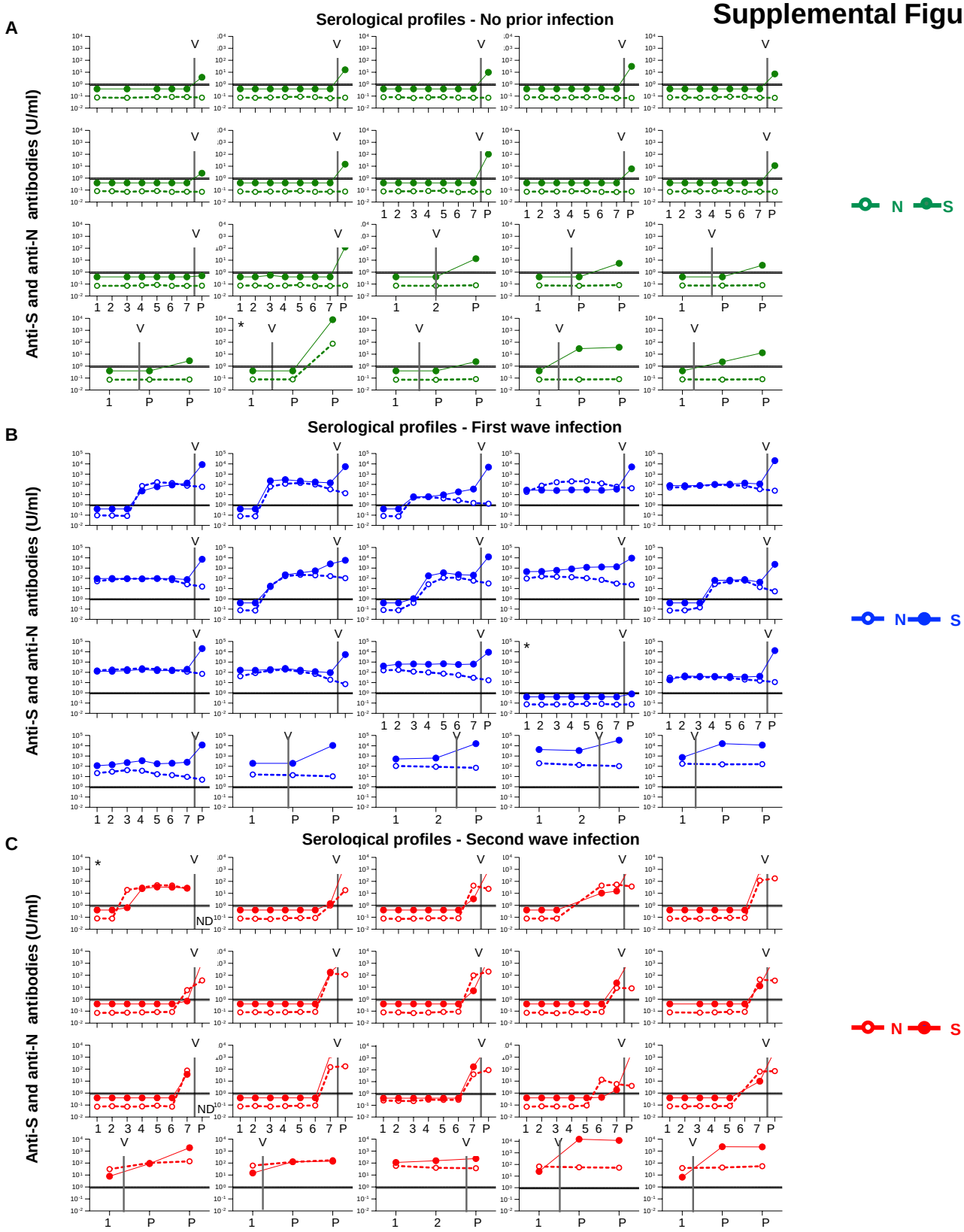

Supplemental Figure 1: Serological profiles of study participants related to Figure 1.
Spike and Nucleocapsid antibody profiles in A. No prior infection group; B. First wave infection; C. Second wave infection group. Serial serum samples were analysed from all available study visits prior to vaccination (3-8 samples per participant). Anti-spike (S; closed circles) and nucleocapsid (N; open circles) antibodies were measured by the Elecsys ECLIA system (Roche Diagnostics). The horizontal lines indicate the cut-off for a positive response (≥0.8 U/mL in the S assay, and ≥1.0 U/mL in the N assay). The vertical line with "v" indicates when vaccination took place. The asterisk indicates a potential breakthrough infection in A (both S and N antibodies increasing after vaccination); a serological non-responder despite a confirmed PCR test for SARS-CoV-2 in B; and a re-infection in C (a positive PCR in the second wave but serological evidence of infection in the first wave). The potential breakthrough and re-infection participants were excluded from further study. In B, 9 participants with the longer observation period were infected prior to the baseline sample (median 42 days, IQR 27-44) in July/August 2020.

Supplemental Figure S2

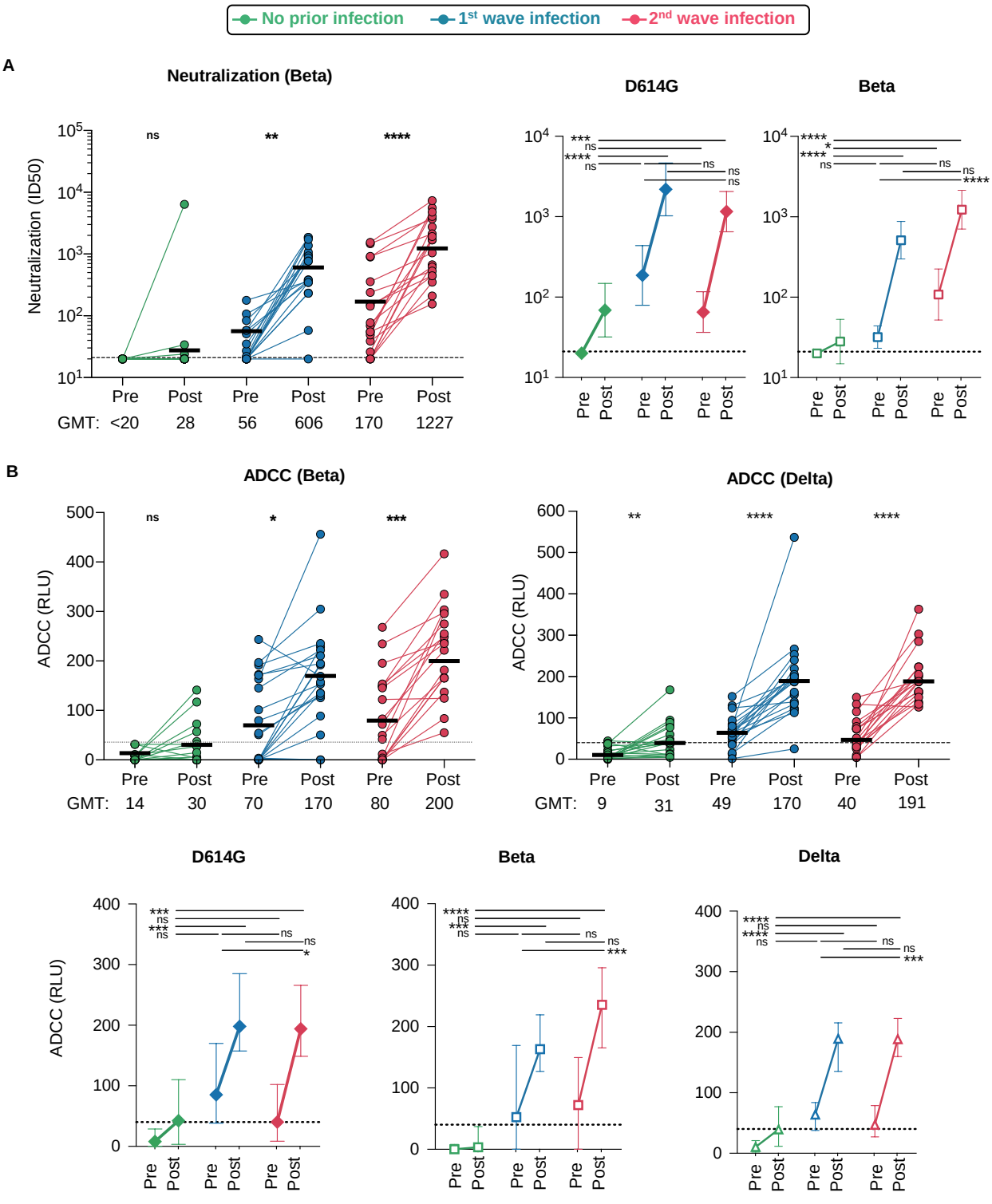

Supplemental Figure 2: Neutralization and ADCC activity pre and post vaccination relating to Figure 2 and 3
A. Neutralization of the SARS-CoV-2 Beta pseudovirus by plasma pre- and post-vaccination from participants with no prior infection (green, n=19) and those infected in the first (blue, n=20) and second waves (red, n=19). Neutralization is reflected as an ID50 titer. The threshold for positivity is indicated by a dotted line and GMT indicated below the graph and as bold black bars. Significance between pre and post vaccination was calculated by the Wilcoxon test. GMT pre and post vaccination are represented against D614G and Beta for each group, with significant represented by a Kruskal-Wallis test with Tukey correction. B. ADCC activity pre and post vaccination against Beta and Delta are shown as relative light units (RLU) with GMT represented below graphs and as before-after plots against D614G, Beta and Delta. * denotes p<0.05, ** p<0.01, *** p<0.001, ****<0.0001 ns, non significant. Experiments were performed in duplicate with the average value shown.

Supplemental Figure S3

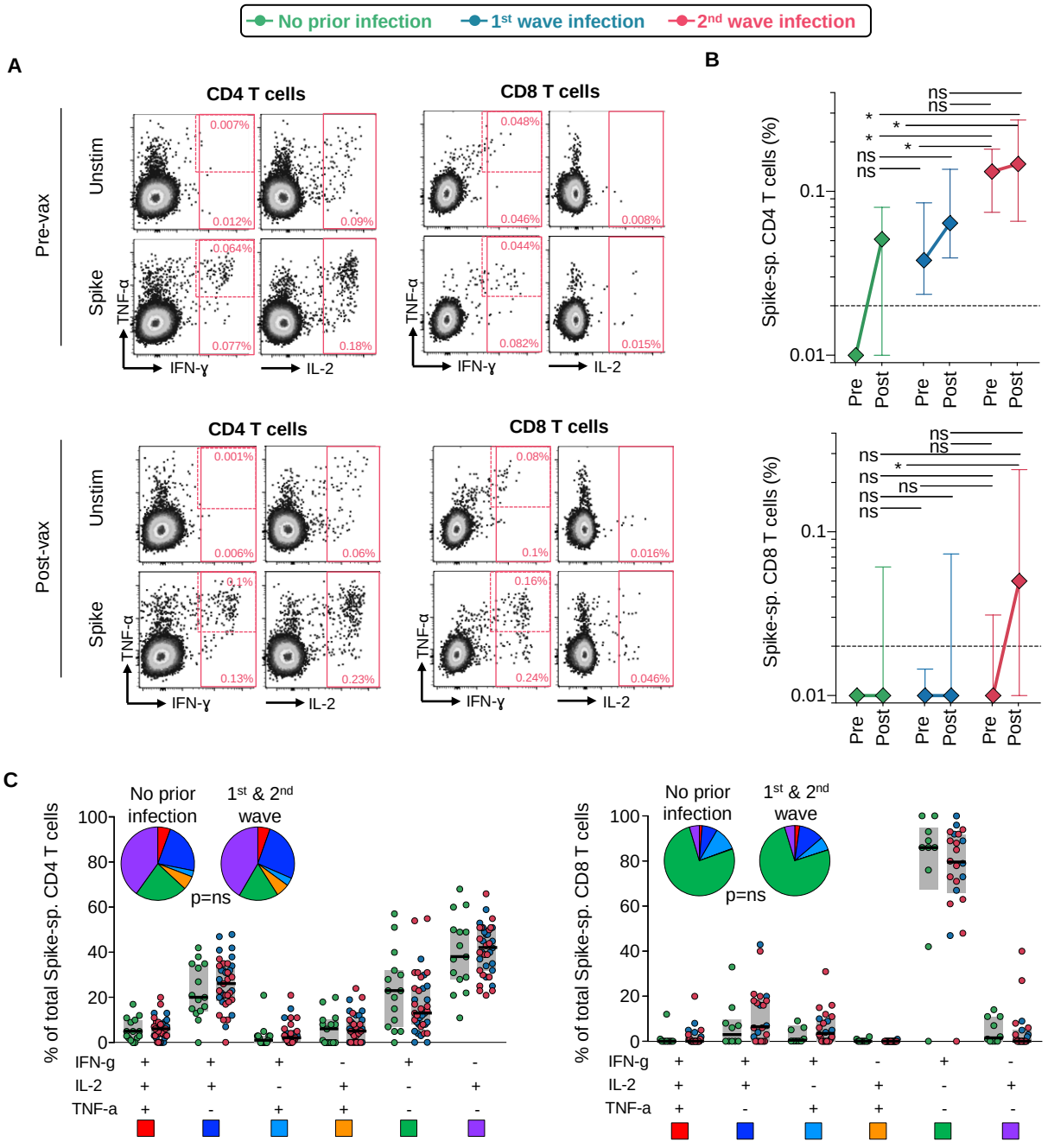

Supplemental Figure 3: Analysis of T cell responses after Ad26.COV2.S vaccination relating to Figure 4.
A. Representative flow cytometry plots of CD4 and CD8 T cell cytokine responses (IFN-g, TNF-a and IL-2) in response to a pool of spike peptides, with the unstimulated control shown. The pre- and post-vaccination plots are shown, from one second wave participant. T cell responses were calculated from boolean gates of all cytokines and the background (unstimulated sample) was subtracted. The single TNF-a-producing subset was excluded due to high background responses. B. Summary of median frequencies of cytokine-producing spike-specific CD4 and CD8 T cells, in those with no prior infection (green, n=19), infection in the first wave (blue, n=20), and infection in the second wave (red, n=19). Symbols represent medians and error bars IQR. Statistical comparisons between groups were performed with the Kruskal Wallis test with Dunn's multiple comparisons test. C. Polyfunctional analysis of CD4 and CD8 T cell responses post-vaccination. Comparison of the polyfunctional profile of spike-specific CD4 T cells (left panel) and CD8 T cells (right panel) in those without prior infection and those previously infected (first and second wave plotted together). Data are expressed as the proportion of each cytokine combination of the total response for each individual. The median and IQR are shown. Each response pattern is color-coded, and summarized in the pie charts. * denotes $p<0.05$, ns = non-significant.